Optical Properties of Nanowires Based on a Blend of Poly (9,9-dioctylfluorene) [PFO] and poly(9,9-dioctyl fluorene-alt-benzothiadiazole) [F8BT].

G. E. Khalil[1,2,3,*], A. M. Adawi [1,4], D. G. Lidzey[1,**]

1. Department of Physics and Astronomy, University of Sheffield, Hicks Building, Hounsfield Road, Sheffield S3 7RH, United Kingdom
2. Physics Department, College of Science, Jouf University, P. O. 2014, Sakaka, Saudi Arabia
3. National Institute for Laser Enhanced Science (NILES), Cairo University, Cairo, Egypt
4. Present address: Department of Physics and Mathematics, University of Hull, Cottingham Road, Hull, HU6 7RX, United Kingdom

* E-mail: G.khalil@niles.edu.eg

** Author to whom correspondence should be addressed:

E-mail:- d.g.lidzey@sheffield.ac.uk

Abstract

Near-field and far-field optical microscopy are used to study the optical properties of nanowires based on a blend of 95% poly (9,9-dioctylfluorene) [PFO] doped with 5% poly (9,9-dioctylfluorene-alt-benzothiadiazole) [F8BT]. Single nanowires were imaged and optical investigations revealed that they act as nanoscale optical waveguides. Investigation using polarization-resolved far-field PL spectroscopy revealed emission from the nanowires was strongly anisotropic having preferred axial polarization. This suggests that a significant number of the polymer chains are oriented along the nanowire axis.

Keywords; Polarization-resolved PL spectroscopy**,** Nanodevices, Organic semiconductors, Optical waveguide, Nanowire, Near and Far-field PL spectroscopy.

I Introduction

Semiconductor nanowires are promising candidates in future nano-photonic and nano-electronic technologies such as photodetectors, lasers and electroluminescent diodes [1, 3-8]. It is anticipated that one-dimensional structures can have electronic properties that are different from those in the bulk materials. This is due to their geometry-reduced size. For example, nanowires exhibit significant anisotropic properties such as fluorescence polarization and directional charge transport along the nanowire axis [3, 4, 9-11]. Semiconductor nanowires based on conjugated polymers form an important class of semiconductor nanowire and can potentially be used as building blocks for nanodevices such as light emitters and waveguides [3-5, 7, 11-13]. In such structures, molecular orientation plays a crucial role since the electrical dipole on a conjugated polymer is aligned along the molecular backbone. Alignment of the polymer backbone along the nanowire axis can be achieved by selection of the appropriate processing parameters such as annealing temperature, the type of solvent used, and molecular weight [14]. Several techniques have been used to fabricate organic nanowires, including self-assembly [15], electrospinning [16], and polymerization in nanoporous templates [17]. Recently, a simple new technique based on wetting of a nano-porous template has been developed for the fabrication of organic nanowires having uniform size [18]. Here, a polymer melt is placed on a porous template. The porous template is then heated to a temperature above polymer glass transition temperature or melting point to facilitate the motion of polymer melt into the template pores. Subsequent controlled cooling results in solidification of the polymer within the template pore walls to form nanowires having a well-defined wall thickness [4, 18]. Alternatively, a drop of a polymer solution is deposited onto the top of porous template. After solvent evaporation, a thin wetting film covers the pore walls forming the polymer nanowires.

The resulting nanowires formed by either method can be released by soaking the polymer-filled template in aqueous NaOH solution for a few hours. Finally, the free nanowires are purified by washing with deionized water and then suspended in a liquid in which the polymer is insoluble [10, 13].

Redmond and co-workers have used this technique to fabricate conjugated polymer semiconductor nanowires [3, 4, 6, 9-11, 13, 19, 20]. Optical spectroscopic studies of polymer nanowires revealed that the photoluminescence from individual nanowire was anisotropic with nanowire emission having a preferred axial polarization.

In this paper, we explore the optical properties of nanowires composed of PFO doped with 5% of F8BT using far field optical microscopy. These nanowires were synthesised by the Nanotechnology Group at Tyndall National Institute (Ireland) using the wetting of nano-porous alumina membrane templates. The use of a blend of polymers allows an exploration of the relative efficiency of energy transfer (via Förster transfer) from PFO to F8BT. Such blends have been used in efficient organic light emitting diodes (LEDs). Here, the combination of phase-separated materials can be used to both increase the PL quantum efficiency and balance electron and hole mobilities [21, 22]. For this reason PFO:F8BT nanowires are of potential interest as building blocks for new organic optoelectronic technologies, such as nanoscale organic light emitting diodes. Here, we show that the nanowires act as active optical waveguides whereby the waveguided PL emission propagates along the nanowire and out-couples at the wire ends, with efficient optical outcoupling being an important property of any system used in a light emitting optoelectronic device. Our measurements using far-field polarization-resolved PL spectroscopy revealed a strong axial polarization anisotropy from the nanowires, which we attribute to the molecular

alignment of PFO and F8BT within the nanowire. Our results suggest therefore that PFO:F8BT nanowires could be used as building blocks in organic nanodevices, by – for example – acting as optical waveguides or sources of polarised light.

II Experimental methods

Absorption spectra were recorded with Horiba Jobin Yvon Fluoromax-4 spectrofluorometer, which covered a spectral range of 200 to 1000 nm. To investigate optical properties of PFO:F8BT nanowires, nanowires mats were deposited onto 0.2 mm glass coverslip from a dilute aqueous suspension. Here, isolated single nanowires were well separated from each other by a few microns. For spectroscopic measurements, each film was mounted into a continuous flow, cold finger helium cryostat held at 4K under a vacuum better than 10^{-5} mbar. In all cases, spectra were acquired under horizontally polarized excitation at 442 nm at both room temperature and 4 K using far-field spectroscopy as described previously [23, 24]. The emission from nanowires were collected at wavelengths above 450 nm. A home built microscope was used to image the fluorescence from the isolated single nanowires, with a series of isolated emitting 'spots' having a typical surface density 0.01 μm^{-2} observed [23].

To acquire polarization dependent PL spectra, a half-wave plate and polarizer were used to control the polarization of the excitation laser and select the polarization of the detected PL. The polarization of the excitation laser was varied and the PL emission from the nanowire was recorded parallel and perpendicular to its long-axis, as described previously [23, 24].

Individual nanowires were imaged using a commercial SNOM (Aurora III from Veeco Instruments, USA) [25, 26], using near-field delivery and far-field

collection. A diode laser was used to excite the sample at 405 nm via the SNOM probe with PL emission being collected in transmission using a microscope objective lens. The PL emission intensity of the individual nanowires at different wavelengths can be measured over a length scale of ~ 100 nm [25, 26].

III Results

Figure 1 shows a tapping mode AFM image of a series of isolated single nanowires. It can be seen that the nanowires are symmetric about their long axis. The individual nanowires were found to have diameters between 200 to 300 nm, reflecting the inhomogeneity of internal diameter of the template pores. The length of the nanowires (L) ranged between 1.4 μm to 20 μm, but for majority of nanowires $L \approx 2$ μm.

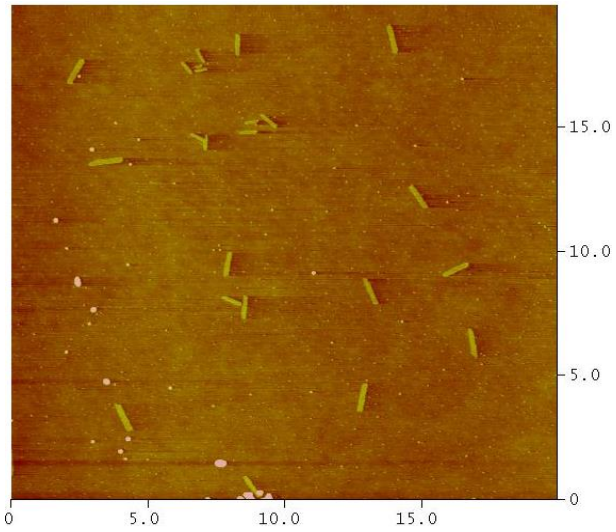

Figure 1. A 20 x 20 μm tapping mode AFM image of PFO:F8BT 95:05 nanowires.

Figure 2(a) shows the normalized absorption and fluorescence emission spectra acquired for a 95:05 PFO:F8BT blend thin film at room temperature. For

comparison, Figure 2 (b) plots the absorption and PL emission from pristine PFO and F8BT films at room temperature.

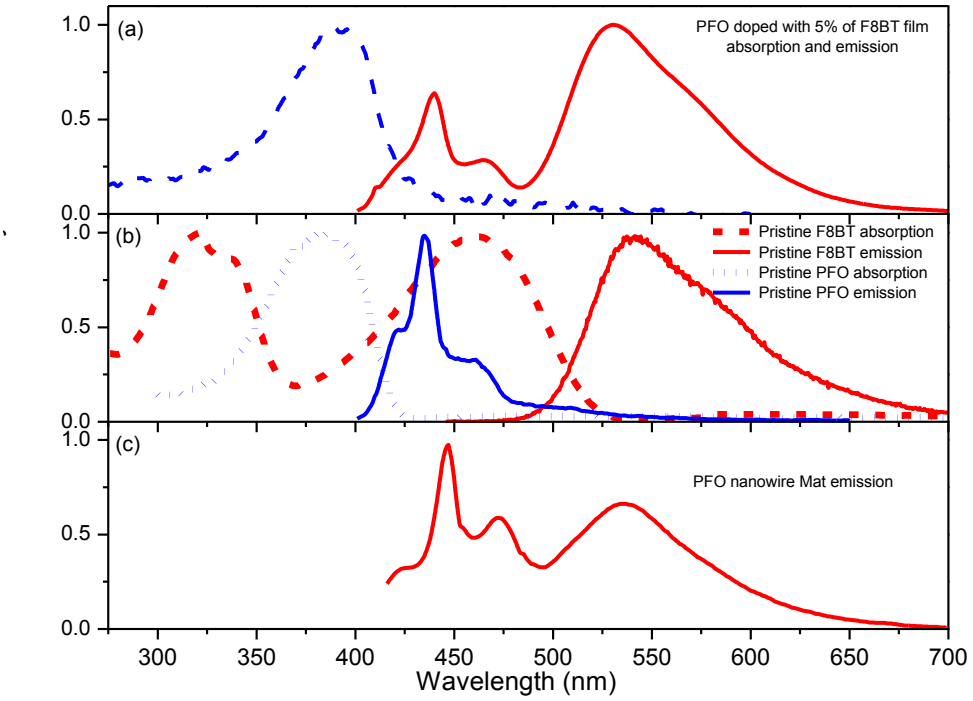

Figure 2. Normalized absorption and fluorescence spectra of (a) a thin film of PFO doped with 5% F8BT by mass (b) a pristine PFO thin film (blue dashed and solid line, respectively) and a pristine F8BT thin film (red dashed and solid line, respectively). (c) Normalized PL spectra of nanowires based on a 95:05 blend of PFO:F8BT deposited onto 0.2 mm glass coverslip from a dilute suspension.

As can be seen, the pristine PFO absorption is characterized by a broad peak at 384 nm. This peak corresponds to the inhomogeneously broadened $S_0 \rightarrow S_1$ transition. Since the blend film contains 95 % PFO polymer, its absorption is similar to that of pristine PFO and peaks at 393 nm, with an additional weaker, long wavelength absorption tail that extends to 525 nm. Due to the large overlap of the PL emission of PFO with F8BT absorption, efficient Förster energy transfer occurs from PFO to F8BT. This can be seen in the PL spectra of the blend film and the nanowire mat.

It can be seen that the PL spectrum of the blend film is dominated by the emission from F8BT at 537 nm, but contains a significant fraction of the PFO emission with peaks located at 440 and 466 nm (corresponding to different vibrational transitions). In comparison with the blend film emission, the PL spectrum acquired from the nanowire mat is red-shifted by 7 nm and exhibits slightly narrower emission peaks as shown in Figure 2(c). It is possibly that this red-shift and spectrum narrowing may result from a narrowed and extended distribution of conjugation lengths. As can be seen, the PL spectrum of the nanowire mat is dominated by PFO emission with relatively weaker emission observed from F8BT, suggesting that energy transfer from PFO to F8BT is relatively suppressed.

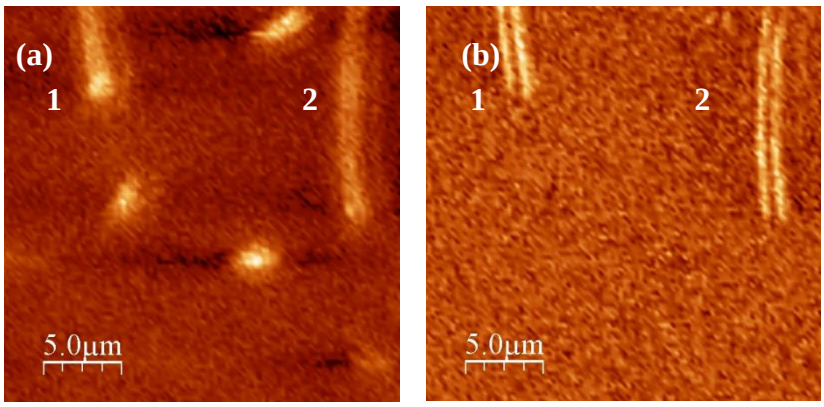

Figure 3. A fluorescence image of individual PFO:F8BT nanowires following excitation at 405 nm. Part (a): A bandpass optical filter (± 20 nm) centred at 550 nm was used to selectively detect the F8BT PL emission from the nanowire. Part (b) A bandpass optical filter (± 20 nm) centred at 450 nm was used to selectively detect the PFO PL emission from the nanowire.

Near-field excitation at 405 nm was used to excite the 95:05 PFO:F8BT nanowires at room temperature. The PL emission from the individual nanowire was

split into two equal parts. A bandpass optical filter (± 20 nm) centred at 450 nm was inserted into one optical path to selectively detect the PFO PL emission from the nanowire (Figure 3 (b)), while a ± 20 nm bandpass filter centred at 550 nm inserted in the other path to detect the F8BT PL emission part from the nanowire (Figure 3 (a)). As can be seen in figure 3, green is emission (characteristic of F8BT) is observed from the interior of two nanowires (labelled as 1 and 2) along with brighter green emission from the tip of nanowire 1. In contrast, blue emission (characteristic of PFO) is only observed from the edges of the nanowires. This suggests that waveguiding of longer wavelength F8BT emission is efficient in such structures with such light being able to escape from the ends of the nanowire, whilst the shorter wavelength emission from PFO is rapidly re-absorbed, with waveguiding being relatively suppressed.

The fluorescence images and spectra for isolated single 95:05 PFO:F8BT nanowires were measured at both room temperature and 4 K using far-field spectroscopy [23, 24]. The nanowires were excited using horizontally polarized excitation at 442 nm with emission collected at wavelengths above 450 nm. In this study, the emission spectra of more than 100 individual, isolated nanowires were acquired.

A typical 28 x 28 μm fluorescence image of individual nanowires with different orientations is shown in Figure 4(a). In Figure 4(b) and (c), we plot a series of typical fluorescence spectra recorded from individual nanowires at room temperature and 4K respectively. Fluorescence spectrum for each nanowire is represented by a line of different colour. Here, all PL spectra are normalized to F8BT PL peak at 540 nm. In these measurements, the PL emission was collected from a region at the centre of each nanowire whose area was approximately 0.4 μm^2. We find that most (~ 85%) of these nanowires have an emission spectrum dominated by F8BT

emission around 540 nm. However, weaker emission is also present around 473 nm (characteristic of PFO). A small subset (~ 15%) of nanowires however have an emission spectrum completely dominated by blue PFO emission.

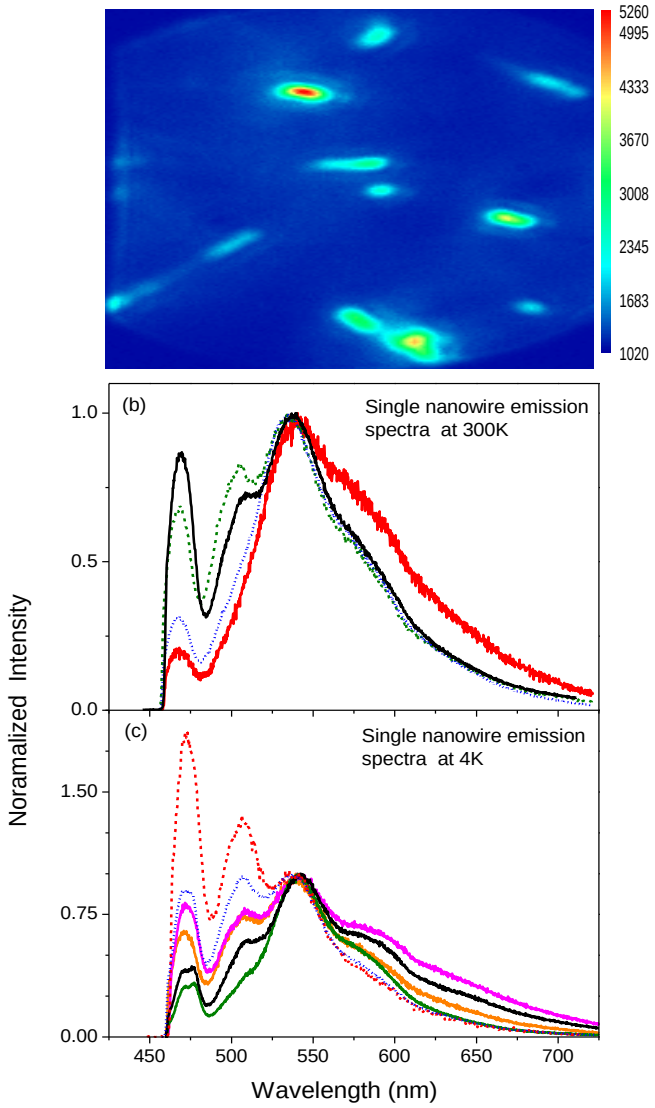

Figure 4. (a) A real-space 28 x 28 μm fluorescence image of a series of individual PFO:F8BT nanowires. (b) and (c) a series of typical fluorescence spectra recorded from individual nanowires at room temperature and at 4K respectively. Fluorescence spectrum for each nanowire is represented by a line of different colour.

As can be seen, the vibronic peaks of individual PFO:F8BT nanowires are better resolved at 4 K compared to room temperature. Specifically, emission around 473 nm (characteristic of PFO) has a linewidth (full width half maximum) of around

16 nm (90 meV) at 4 K and 19 nm (106 meV) at 300 K. This observed spectral narrowing and red shift compared with room temperature emission can be explained by a reduction in thermally-induced disorder which increases molecular conjugation length and decreases the energy-gap [27, 28].

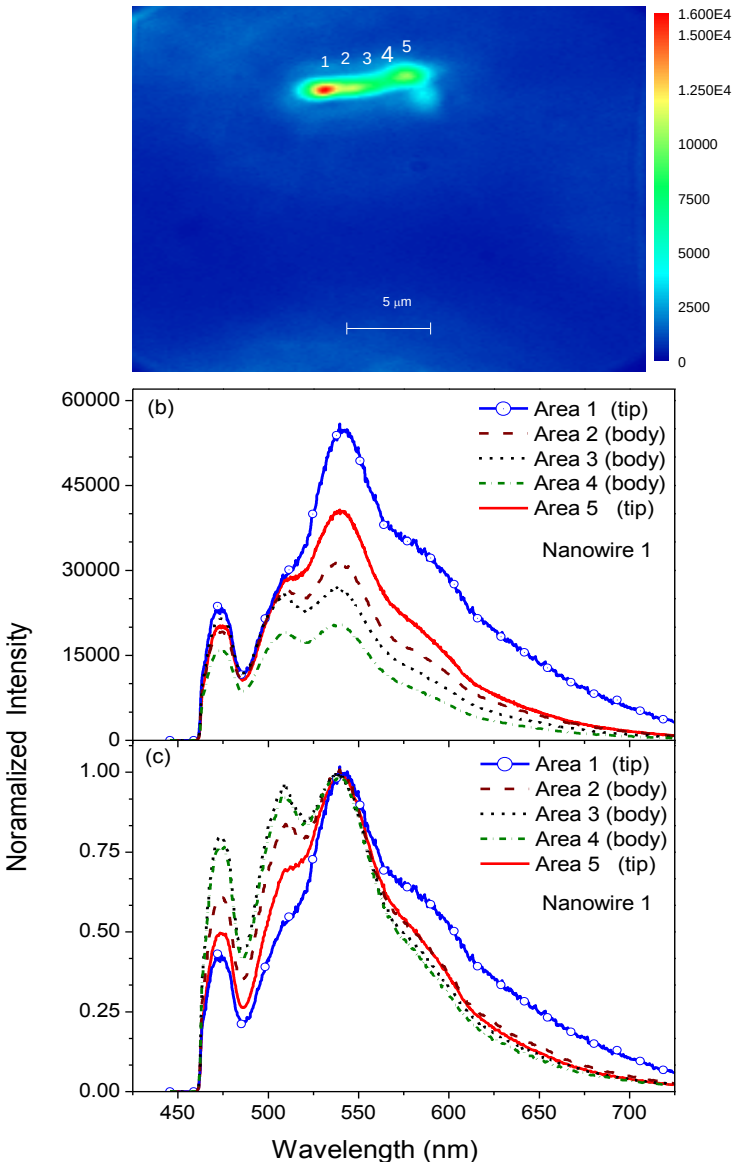

Figure 5. **(**a) 28 x 28 µm fluorescence image of a single nanowire. (b) PL spectra acquired at various points along the nanowire. (c) PL spectra normalized to F8BT emission.

Our measurements indicate that the PL intensity varies significantly along each nanowire. Furthermore, we find that there is a significant variation in the relative intensity between the blue PFO emission (peaks observed at 473 and 508 nm) and the

green F8BT emission peaking at 541 nm. Data taken from one such nanowire, (about 6 μm in length), is illustrated in Figure 5. A notable bright spot (region 1) is observed at the leftmost tip of the nanowire (part (a)). However, the emission from the rightmost tip (region 5) of the nanowire was less intense. PL spectra were acquired at several positions along nanowire long-axis as shown in Figure 5(b). These spectra are plotted again in part (c), but are normalized to the emission peak at 541 nm, which is characteristic F8BT. Here, the emission was collected in a direction perpendicular to nanowire long axis using an objective lens whose collection cone angle is ~ 50°.

Previous studies on organic and inorganic nanowires have highlighted the importance of the transition dipole moment orientation in determining emission properties [20, 29]. As the molecules most strongly absorb and emit photons whose polarization is oriented parallel to the orientation of their transition dipole, polarization can be used as a probe of molecular alignment, as in most cases the transition dipole moment in a polymer is aligned parallel to the molecular chain axis [30]. We have therefore used far-field polarization resolved PL spectroscopy to investigate the emission polarization from 95:05 PFO:F8BT nanowires.

The polarization resolved PL spectra of a typical nanowire is shown in Figure 6. Here, the PL spectra were collected from four different regions along the nanowire. Parts (b) to (e) show the PL emission acquired for vertically-polarized excitation (parallel to nanowire long-axis) and collected using either vertical (VV) or horizontal (VH) polarizations. Parts (f) to (i) show the PL emission spectra for the same nanowire acquired following horizontally polarized excitation and collected at both horizontal (HH) and vertical (HV) polarizations. Regardless of the polarization excitation, our measurements indicate that each nanowire emits most emission polarized parallel to its long-axis.

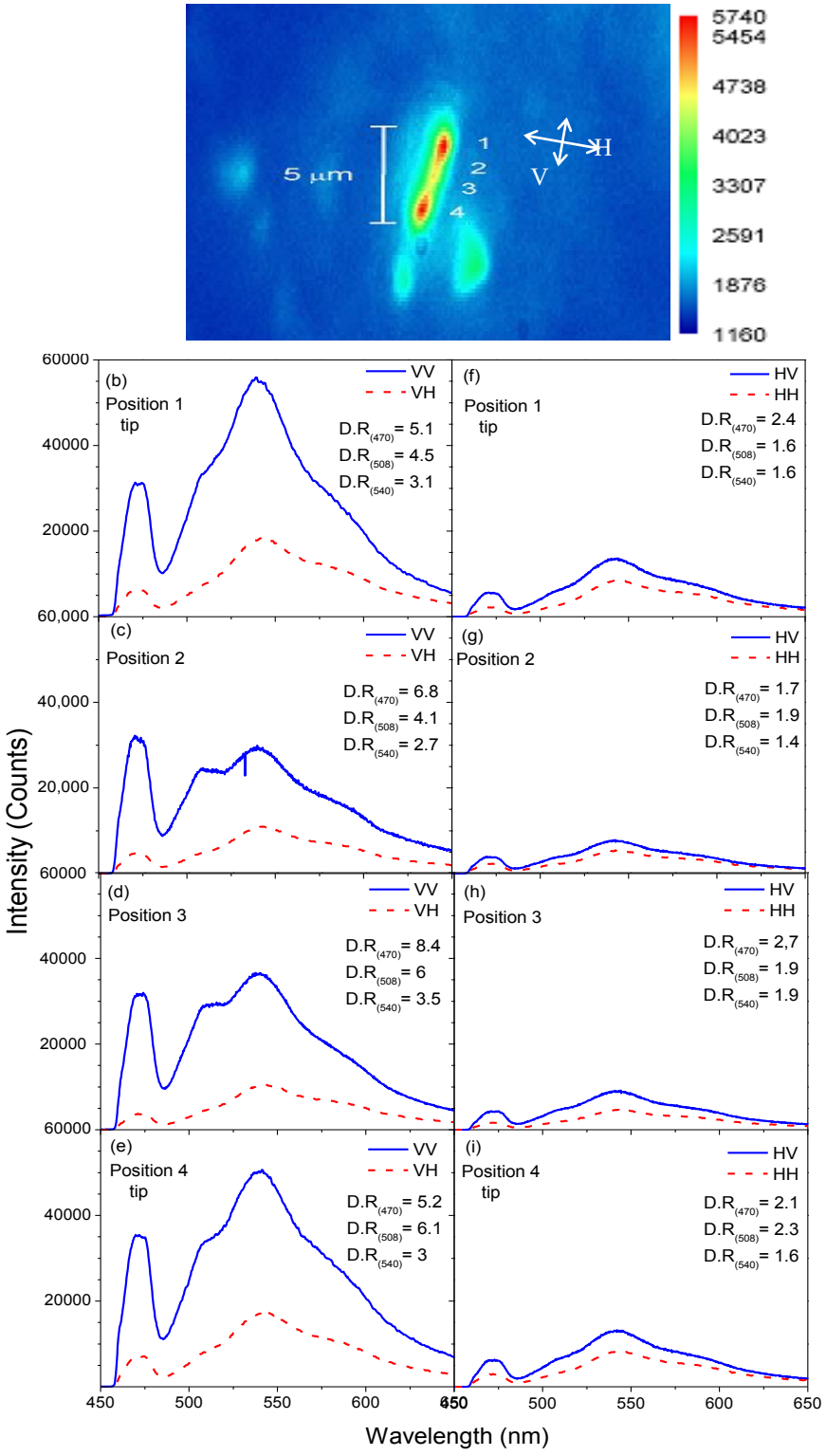

Figure 6. (a) Fluorescence image of a 5 µm long nanowire. Parts (b) to (e) show polarization resolved PL spectra acquired at various positions along the nanowire long axis following vertically polarized excitation. Parts (f) to (i) show polarization resolved PL spectra acquired at various positions along the nanowire long axis following horizontally polarized excitation.

IV Discussion

In general, there are several possible causes for spatial variations in PL intensity along a nanowire. One possibility is that there is a variation in the nanowire diameter. This could be result from variations in the internal diameter of the template pores and to defects within each pore [19]. Other possible reasons are the presence of impurities, or insoluble clumps of polymer molecules protruding from the nanowire surface [31].

SNOM fluorescence images for isolated single 95:05 PFO:F8BT nanowires in Figure 3 reveal blue PFO emission from nanowire edges along with green F8BT emission from the interior of the nanowire and strong bright green F8BT emission from nanowire tips. This suggests that the nanowires function as nanoscale optical waveguides whereby the green F8BT emission propagates towards and then out-couples at the wire ends. Figure 3 does not provide information about the orientation of polymer chains within the nanowire. Therefore, we have used polarization-resolved far-field PL spectroscopy to measure the alignment and orientation of PFO and F8BT polymer chains within the nanowire.

A large number of nanowires studied seem to have stronger emission from their tip compared to nanowire body under all polarization conditions, as shown in Figures 5 and 6. Furthermore, we find that the residual blue PFO emission (at 473 and 508 nm) is weaker when detected at the nanowire tips.

As the blue PFO emission is expected to be strongly absorbed in the nanowire, it suggests that the enhanced green emission from the nanowire tips actually results from waveguided green emission (which is weakly absorbed) and therefore scattered out of the nanowire ends. Such optical waveguide behaviour most probably results from the significant difference in refractive index between the nanowire ($n_{nw} \approx 1.8$)

[32] and its surroundings ($n_S \approx 1.5$ for substrate, and $n_0 = 1.0$ for air). Such behaviour is similar to that previously observed in fluorene-based organic nanowires [4, 9, 13, 33] and inorganic nanowires [34-36], whereby the resulting PL emission propagates along nanowire long-axis and out-couples at the tip.

The PL out-coupled at a nanowire tip has a divergence angle (θ) given by

$$\theta = arctan\left(\frac{2\lambda}{\pi d}\right) \qquad 1$$

where λ is the emission wavelength and *d* is the diameter of the nanowire. For a 300 nm diameter nanowire, the expected divergence angle of the emission at 473 and 540 nm is 44° and 49° respectively. As the PL spectra were collected at angle of 90° with respect to nanowire long axis, the portion of outcoupled emission directed towards the collection objective lens will depend strongly on the tip morphology [9]. As can be seen in Figure 5, there is a slight bend near the rightmost tip of the nanowire. As a result, part of emission may be lost at such bend leading to less intense outcoupled emission at the rightmost tip of the nanowire. The difference in the morphology of two end facets of the nanowire may be also a reason for their relative difference in PL intensity.

The waveguide behaviour of a nanowire depends on the emission wavelength and the orientation of the emission dipole within the nanowire [29]. For cylindrical waveguide, the fractional guided mode power is given by

$$\eta = 1 - \left(2.4\, exp\left[-\frac{1}{V}\right]\right)^2 V^{-3} \qquad 2$$

where $V = (\pi d/\lambda)\left(n_{nw}^2 - n_0^2\right)^{1/2}$ and n_{nw} and n_0 are the refractive index of the nanowire and air respectively. For a 300 nm diameter 95:05 PFO:F8BT nanowire, we calculate

that 89% of optical power will be confined within the core for light at 473 nm, which drops to ~ 85% at 540 nm. This suggests higher propagation losses for the green part of the emission, possibly due to weaker coupling to waveguide modes [9, 13, 29].

Waveguide behaviour has not been observed in all nanowires. For some nanowires, this could be attributed to the variation in their diameter, the presence of structural defects, or the degree of substrate coupling, which increases the scattering propagation loss [4, 9, 29]. In addition, it is also likely that in some nanowires, outcoupled emission is diffracted from the tip in a direction away from the collection objective.

It can be seen that the nanowire emission is strongly anisotropic with a maximum emission intensity observed when the excitation and resulting PL emission are both polarized parallel to nanowire long-axis (VV). A distinct minimum intensity is similarly detected for both polarizations perpendicular to the nanowire long-axis (HH). This axial emission polarization suggests that a significant number of the emissive polymer molecules and hence their emission transition dipoles are aligned parallel to the nanowire long-axis. However, it is clear that there is nonzero emission intensity observed at both horizontally polarized excitation and collection. This suggests that the alignment of the polymer chains along the nanowire long-axis is not complete. This non-negligible horizontally polarized emission may result from several factors:

(i) The emission transition dipoles make angles ~ 26.5° and ~ 22° relative to the chain axis for PFO and F8BT, respectively [37, 38]. These slightly off-axis angles limit the PL emission anisotropy.

(ii) There may be a distribution of polymer chain orientations with respect to the nanowire long-axis.

(iii) Excitons are able to migrate between molecular chains having different orientations within the nanowire.

(iv) Light scattered from the substrate and impurities may also reduce the PL emission anisotropy.

To quantify the polarization anisotropy and explore these possibilities we have estimated the relative emission anisotropy at different peaks that appear in nanowire emission spectra using

$$DR_i = \left(I_{iV} / I_{iH}\right). \qquad .3$$

Here I is the intensity of emission, with subscripts $i = V$ or H signifying vertically (parallel to nanowire long-axis) or horizontally (perpendicular to nanowire long-axis) polarized excitation. For each polarization condition, the emission polarization ratio (ρ) is given by [14, 39]

$$\rho = \left(\frac{I_{iV} - I_{iH}}{I_{iV} + I_{iH}}\right) = \left(\frac{DR_i - 1}{DR_i + 1}\right). \qquad 4$$

The emission dichroic ratio (DR_i) and emission polarization ratio (ρ) were determined at a wavelength corresponding to the different peaks that appear in nanowire emission spectra. Regardless of excitation polarization, DR (and therefore ρ) were found to vary along the nanowire as shown in Figure 6. For vertically polarized excitation, the calculated emission polarization ratios at 473 and 540 nm varied from ρ = 0.67 to 0.79, and 0.46 to 0.56, respectively. However, for horizontally polarized excitation, ρ varied from 0.26 to 0.46, and 0.17 to 0.31

respectively. The values of ρ determined at 473 nm are very close to previously reported values (from 0.64 to 0.83) for PFO nanowires. These large values for ρ have been attributed to the preferential axial alignment of PFO polymer chains [14].

Since the off-axis transition dipole moment on F8BT is smaller than that of PFO [37, 38], ρ-values are expected to be larger at 541 nm, characteristic for F8BT, than at 473 nm, characteristic for PFO, emission peaks. However, the data in Figures 6 suggest smaller ρ-values at 541 nm emission peak. This can be also clearly seen in Figure 7, where we plot the average emission polarization ratio for 16 nanowires as a function of PL emission wavelength for both horizontally and vertically polarized excitation. This decrease in emission anisotropy at longer wavelength suggests that there is a greater degree of chain alignment of PFO than F8BT along the nanowire long-axis.

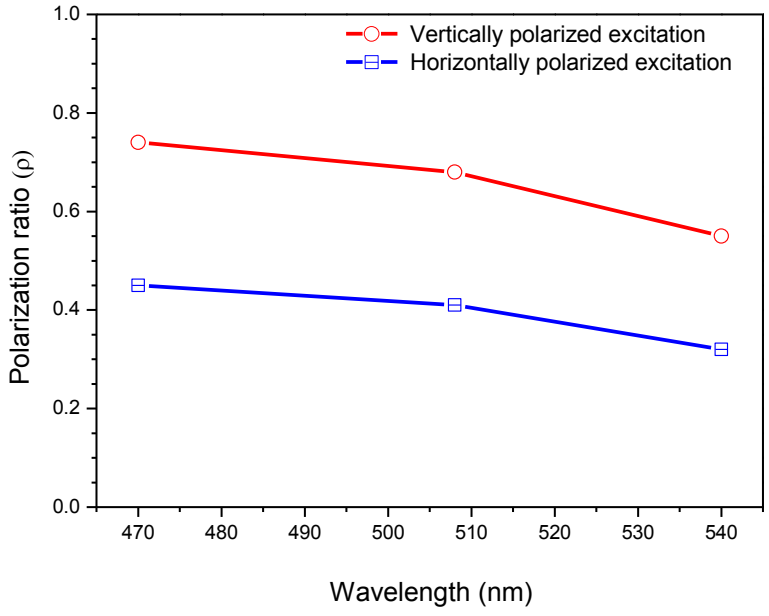

Figure 7. Average polarization ratio as a function of emission wavelength.

Emission polarization anisotropy values up to 0.96 have been reported for inorganic nanowire waveguides [40]. Such high values have been attributed to the large dielectric contrast between the nanowire and its surroundings. Dielectric confinement effects only occur in homogenous nanowires having a dielectric constant that is larger than the surrounding medium (i.e. $\varepsilon_{nw} \rangle\ \varepsilon_0$) and a diameter that is much less, and a length that is much greater than the excitation wavelength (d $\langle\langle\ \lambda_{exc}$). Under such conditions, when the excitation is polarized parallel to nanowire long-axis, the power confined within the nanowire is not reduced. However, for excitation polarized perpendicular to nanowire long-axis, the confined intensity is attenuated according to [40]

$$I_c = \left(\frac{2\varepsilon_0}{\varepsilon_{nw} + \varepsilon_0} \right)^2 I_0 \qquad 5$$

where I_c is the confined intensity and I_0 is the excitation intensity. If the anisotropic optical properties of 95:05 PFO:F8BT nanowires originate from dielectric confinement effects, an emission polarization ratio of 0.64 would be expected. However, since the nanowires studied have a diameter slightly smaller than the excitation wavelength ($d/\lambda \approx 0.6$), dielectric confinement effects are unlikely to be the dominant mechanism for the observed polarization emission anisotropy. This suggests that it is the emission transition dipole moments of PFO and F8BT within the nanowire backbone that accounts for the observed polarization emission anisotropy.

V Conclusions

Optical spectroscopy of nanowires composed of a 95:05 blend of PFO:F8BT revealed that they act as nanoscale optical waveguides whereby the waveguided PL emission propagates along the nanowires and out-couples at the wire ends. This is evidenced by the attenuation of the short-wavelength PL emitted from the tip compared with that from the body; an effect that points towards the reabsorption of waveguided PL during propagation along the nanowire.

Single nanowire far-field polarization-resolved emission revealed a strong axial polarization, suggesting that most PFO and F8BT molecules are aligned parallel to the nanowire axis. Although the off-axis transition dipole moment of F8BT is smaller than that of PFO, the measured anisotropy values were smaller at 541 nm (characteristic of F8BT) than at 473 nm (characteristic of PFO). This effect most likely results from F8BT molecules having a reduced degree of alignment with respect to nanowire long-axis compared with PFO.

Acknowledgements

We are most grateful to Prof. Gareth Redmond at University College Dublin and to Nanotechnology Group at Tyndall National Institute University College Cork, Ireland for nanowire synthesis.

References

[1] D.J. Sirbuly, M. Law, H. Yan, P. Yang, Semiconductor nanowires for subwavelength photonics integration, The Journal of Physical Chemistry B, 109 (2005) 15190-15213.

[2] W. Lu, C.M. Lieber, Semiconductor nanowires, Journal of Physics D: Applied Physics, (2006) R387.

[3] G.A. O'Brien, A.J. Quinn, D.A. Tanner, G. Redmond, A Single Polymer Nanowire Photodetector, Advanced Materials, 18 (2006) 2379-2383.

[4] D. O'Carroll, I. Lieberwirth, G. Redmond, Microcavity effects and optically pumped lasing in single conjugated polymer nanowires, Nat Nano, 2 (2007) 180-184.

[5] S. Oh, R. Hayakawa, T. Chikyow, Y. Wakayama, Nanochannel effect in polymer nanowire transistor with highly aligned polymer chains, Applied Physics Letters, 106 (2015) 243301.

[6] C. Zhang, C.-L. Zou, H. Dong, Y. Yan, J. Yao, Y.S. Zhao, Dual-color single-mode lasing in axially coupled organic nanowire resonators, Science Advances, 3 (2017) e1700225.

[7] H. Xia, T. Chen, C. Hu, K. Xie, Recent Advances of the Polymer Micro/Nanofiber Fluorescence Waveguide, Polymers (Basel), 10 (2018).

[8] H. Xia, C. Hu, T. Chen, D. Hu, M. Zhang, K. Xie, Advances in Conjugated Polymer Lasers, Polymers, 11 (2019) 443.

[9] D O'Carroll, I Lieberwirth, G Redmond, Melt-processed polyfluorene nanowires as active waveguides, Small, 3 (2007) 1178-1183.

[10] S. Moynihan, D. Iacopino, D. O'Carroll, P. Lovera, G. Redmond, Template synthesis of highly oriented polyfluorene nanotube arrays, Chemistry of Materials, 20 (2008) 996-1003.

[11] P. Lovera, G. Redmond, Colour-coded photoluminescence and chemiluminescence of fluorene polymer-based organic nanowires in random and organised arrangements, J Nanosci Nanotechnol, 13 (2013) 5194-5202.

[12] K. Takazawa, Y. Kitahama, Y. Kimura, G. Kido, Optical waveguide self-assembled from organic dye molecules in solution, Nano Letters, 5 (2005) 1293-1296.

[13] Deirdre O'Carroll, G. Redmond, Polyfluorene nanowire active waveguides as sub-wavelength polarized light sources, Physica E: Low-dimensional Systems and Nanostructures, 40 (2008) 2468-2473.

[14] Deirdre O'Carroll, Gareth Redmond, Highly anisotropic luminescence from poly(9,9-dioctylfluorene) nanowires doped with orientationally ordered β-phase polymer chains, Chemistry of Materials, 20 (2008) 6501-6508.

[15] S. Masuo, H. Yoshikawa, H.-G. Nothofer, A.C. Grimsdale, U. Scherf, K. Mullen, H. Masuhara, Assembling and orientation of polyfluorenes in solution controlled by a focused near-infrared laser beam, The Journal of Physical Chemistry B, 109 (2005) 6917-6921.

[16] A. Babel, D. Li, Y. Xia, S.A. Jenekhe, Electrospun nanofibers of blends of conjugated polymers: morphology, optical properties, and field-effect transistors, Macromolecules, 38 (2005) 4705-4711.

[17] X. Zhang, J. Zhang, W. Song, Z. Liu, Controllable synthesis of conducting polypyrrole nanostructures, The Journal of Physical Chemistry B, 110 (2006) 1158-1165.

[18] M. Steinhart, J.H. Wendorff, A. Greiner, R.B. Wehrspohn, K. Nielsch, J. Schilling, J. Choi, U. Gosele, Polymer nanotubes by wetting of ordered porous templates, Science, 296 (2002) 1997-.

[19] D.I. D. O'Carroll, A. O'Riordan, P. Lovera, ঃ. O'Connor, G. A. O'Brien, G. Redmond,, Poly(9,9-dioctylfluorene) nanowires with pronounced β-phase morphology: synthesis, characterization, and optical properties, Advanced Materials, 20 (2008) 42-48.

[20] D. O' Carroll, J. Irwin, D.A. Tanner, G. Redmond, Polyfluorene nanowires with pronounced axial texturing prepared by melt-assisted template wetting, Materials Science and Engineering: B, 147 (2008) 298-302.

[21] J. Morgado, R. Friend, F. Cacialli, Improved efficiency of light-emitting diodes based on polyfluorene blends upon insertion of a poly(p-phenylene vinylene) electron- confinement layer, Applied Physics Letters, 80 (2002) 2436-2438.

[22] D. de Azevedo, J.N. Freitas, R.A. Domingues, M.M. Faleiros, T.D.Z. Atvars, Correlation between the PL and EL emissions of polyfluorene-based diodes using bilayers or polymer blends, Synthetic Metals, 233 (2017) 28-34.

[23] G.E. Khalil, A.M. Adawi, A.M. Fox, A. Iraqi, D.G. Lidzey, Single molecule spectroscopy of red- and green-emitting fluorene-based copolymers, The Journal of Chemical Physics, 130 (2009) 044903.

[24] G. Khalil, A. Adawi, B. Robinson, A. Cadby, W. Tsoi, J. Kim, A. Charas, J. Morgado, D. Lidzey, Spectroscopy and single-molecule emission of a fluorene-terthiophene oligomer, The Journal of Physical Chemistry B, 115 (2011) 12028-12035.

[25] A. Cadby, R. Dean, A. Fox, R. Jones, D. Lidzey, Mapping the fluorescence decay lifetime of a conjugated polymer in a phase-separated blend using a scanning near-field optical microscope, Nano letters, 5 (2005) 2232-2237.

[26] A. Cadby, G. Khalil, A. Fox, D. Lidzey, Mapping exciton quenching in photovoltaic-applicable polymer blends using time-resolved scanning near-field optical microscopy, Journal of Applied Physics, 103 (2008) 093715.

[27] P.K.H. Ho, J.-S. Kim, N. Tessler, R.H. Friend, Photoluminescence of poly(p-phenylenevinylene)–silica nanocomposites: Evidence for dual emission by Franck–Condon analysis, The Journal of Chemical Physics, 115 (2001) 2709-2720.

[28] Y.-Y. Lin, C.-W. Chen, J. Chang, T.Y. Lin, I.S. Liu, W.-F. Su, Exciton dissociation and migration in enhanced order conjugated polymer/nanoparticle hybrid materials, Nanotechnology, 17 (2006) 1260-1263.

[29] J.C. Johnson, H. Yan, P. Yang, R.J. Saykally, Optical cavity effects in ZnO nanowire lasers and waveguides, The Journal of Physical Chemistry B, 107 (2003) 8816-8828.

[30] S.M. King, H.L. Vaughan, A.P. Monkman, Orientation of triplet and singlet transition dipole moments in polyfluorene, studied by polarised spectroscopies, Chemical Physics Letters, 440 (2007) 268-272.

[31] J. Teetsov, D.A. Vanden Bout, Near-field scanning optical microscopy (NSOM) studies of nanoscale polymer ordering in pristine films of poly(9,9-dialkylfluorene), The Journal of Physical Chemistry B, 104 (2000) 9378-9387.

[32] M. Campoy-Quiles, P.G. Etchegoin, D.D.C. Bradley, On the optical anisotropy of conjugated polymer thin films, Physical Review B, 72 (2005) 045209.

[33] Q. Liao, Z. Xu, X. Zhong, W. Dang, Q. Shi, C. Zhang, Y. Weng, Z. Li, H. Fu, An organic nanowire waveguide exciton–polariton sub-microlaser and its photonic application, Journal of Materials Chemistry C, 2 (2014) 2773-2778.

[34] M. Law, D.J. Sirbuly, J.C. Johnson, J. Goldberger, R.J. Saykally, P. Yang, Nanoribbon waveguides for subwavelength photonics integration, Science, 305 (2004) 1269-1273.

[35] Y. Xiang, J. Chen, D. Zhang, R. Wang, Y. Kuai, F. Lu, X. Tang, P. Wang, H. Ming, M. Rosenfeld, R. Badugu, J. Lakowicz, Manipulating Propagation Constants of

Silver Nanowire Plasmonic Waveguide Modes Using a Dielectric Multilayer Substrate, Applied Sciences, 8 (2018) 144.

[36] D. Zhang, Y. Xiang, J. Chen, J. Cheng, L. Zhu, R. Wang, G. Zou, P. Wang, H. Ming, M. Rosenfeld, R. Badugu, J.R. Lakowicz, Extending the Propagation Distance of a Silver Nanowire Plasmonic Waveguide with a Dielectric Multilayer Substrate, Nano letters, 18 (2018) 1152-1158.

[37] H.-M. Liem, P. Etchegoin, K.S. Whitehead, D.D.C. Bradley, Raman anisotropy measurements: an effective probe of molecular orientation in conjugated polymer thin films, Advanced Functional Materials, 13 (2003) 66-72.

[38] S.A. Schmid, K.H. Yim, M.H. Chang, Z. Zheng, W.T.S. Huck, R.H. Friend, J.S. Kim, L.M. Herz, Polarization anisotropy dynamics for thin films of a conjugated polymer aligned by nanoimprinting, Physical Review B (Condensed Matter and Materials Physics), 77 (2008) 115338.

[39] P.L. Shane Moynihan, Deirdre O'Carroll, Daniela Iacopino, Gareth Redmond,, Alignment and dynamic manipulation of conjugated polymer nanowires in nematic liquid crystal hosts, Advanced Materials, 20 (2008) 2497-2502.

[40] J. Wang, M.S. Gudiksen, X. Duan, Y. Cui, C.M. Lieber, Highly polarized photoluminescence and photodetection from single Indium phosphide nanowires, Science, 293 (2001) 1455-1457.